

Ultrafast band-edge tuning of a two-dimensional silicon photonic crystal via free-carrier injection

S. W. Leonard* and H. M. van Driel

Department of Physics, University of Toronto, 60 Saint George Street, Toronto, Ontario M5S 1A7, Canada

J. Schilling and R. B. Wehrspohn

Max-Planck-Institute of Microstructure Physics, Weinberg 2, D-06120 Halle, Germany

(Received 1 August 2002; published 9 October 2002)

Ultrafast tuning of the band edge of a two-dimensional silicon/air photonic crystal is demonstrated near a wavelength of $1.9 \mu\text{m}$. Changes in the silicon refractive index are optically induced by injecting free carriers with 800 nm, 300 fs pulses. The rise time of the shift occurs on the time scale of the pulse width apart from a small component associated with carrier cooling; the recovery time is related to electron-hole recombination. The band edge is observed to shift linearly with pump beam fluence, with a shift in excess of 30 nm for a pump beam fluence of 2 mJ cm^{-2} . A nonuniform spectral shift is attributed to finite pump beam absorption depth effects.

DOI: 10.1103/PhysRevB.66.161102

PACS number(s): 42.70.Qs, 42.65.Re, 42.79.Ta

Photonic crystals are periodic dielectric materials which continue to generate considerable interest because of their ability to offer novel ways to control the flow of light.¹⁻⁶ This new class of optical materials has led to the demonstration of interesting physical phenomena such as novel waveguiding effects,^{7,8} superprism effects,⁹ and control over spontaneous emission rates.¹⁰ There is clearly a great potential for a new generation of passive and active optical components including new types of integrated optical circuits.

Many of the unusual properties of photonic crystals are based on the existence of a partial or complete photonic band gap, a natural consequence of the material's underlying periodicity. The range of physical phenomena or applications of photonic crystals could be enlarged in scope if these band gaps, or indeed, other characteristics of photonic crystals, could be tuned on very short time scales. In the past, studies of tunable photonic crystals have focused primarily on electro and thermo-optic band-edge tuning via infiltrated liquid crystals.¹¹⁻¹⁴ Unfortunately, the molecular reorientation processes responsible for changes in the refractive index of thermotropic liquid crystals typically occur on time scales ranging from milliseconds to seconds, strictly prohibiting rapid band-edge tuning.

Much faster tunability can only be achieved using electronic processes. Ultrafast changes in the refractive index can occur via nonresonant processes such as the optical Kerr effect, or resonant processes in which free electrons and holes¹⁵ are created. The former effect can induce index changes which follow the light pulse, but requires high light intensities. The latter process requires substantially lower pump intensity and can still lead to induced changes limited by the pulse width. Relaxation should be limited by the carrier recombination time, which can be as short as a picosecond in suitably designed materials.^{16,17} Recently, Halevi and Ramos-Mendieta¹⁸ have theoretically shown how thermally activated carriers can tune two-dimensional photonic crystals fabricated with a narrow gap semiconductor (InSb). Susa¹⁹ has also theoretically studied how the continuous optical injection of free carriers can shift the band edge of a two-dimensional photonic crystal for moderate pumping intensi-

ties. Experimentally, free carriers generated by two-photon absorption have been used to change the refractive index and transmission properties of a Si/SiO₂ dielectric stack (1D photonic crystal).²⁰ However, since the induced transmission changes were quite small ($<0.5\%$) and were measured only at one wavelength, it was not possible to offer many details about the temporal or spectral characteristics of the induced changes. Also, Chelnikov *et al.*²¹ were able to show how free carriers could also control defect mode absorption in a 3D silicon crystal with a photonic gap in the submillimeter range near 250 GHz. Hence, while some preliminary results have been given, very little is known about how optical beams can be used to alter the optical properties of high-dimensional (2D or 3D) photonic crystals, and their band gaps, in particular, in the near infrared region of the spectrum where most applications would be expected to arise.

Here we report the demonstration of ultrafast photonic band-edge tuning in a two-dimensional photonic crystal in the near infrared.²² Optically injected free carriers are used to induce a large $>30\text{-nm}$ band-edge shift on femtosecond time scales. This is done in macroporous silicon photonic crystals, fabricated using the techniques reported in Refs. 23-25. The samples have a triangular lattice of air pores in silicon, with a pitch of 500 nm and a pore radius of 206 nm. The pores extend $100 \mu\text{m}$ in depth and the sample is cleaved perpendicular to the so-called Γ -M direction, as shown in Fig. 1. For this direction, a stop gap occurs from 1.9 to $2.3 \mu\text{m}$; this gap is the focus of this report.

The injection of electron-hole pairs in a semiconductor is known to alter both the refractive index and absorption coefficient via a Drude contribution to the dielectric function.¹⁵ In the absence of significant absorption, the dielectric function can be described by $\epsilon(\omega) = \epsilon_b - \omega_p^2/\omega^2$, where $\omega_p = (Ne^2/\epsilon_0 m^*)^{1/2}$ is the plasma frequency, N is the density of electron-hole pairs, ϵ_b is the dielectric constant of quiescent silicon, m^* is the reduced effective mass and ω is the probe frequency. For our experiments, in which probe light with a wavelength near $1.9 \mu\text{m}$ is used and carrier densities are less than $2 \times 10^{19} \text{ cm}^{-3}$, the imaginary terms in the dielectric function arising from free-carrier absorption and

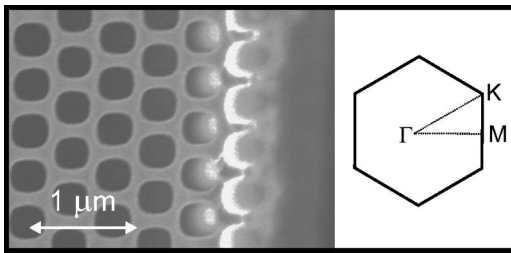


FIG. 1. Scanning electron microscope image of two-dimensional photonic crystal with lattice pitch of 500 nm. The sample has a height of 100 μm and a radius to pitch ratio of $r/a = 0.411$. Inset, first Brillouin zone of triangular lattice.

intervalence-band absorption are very small.²⁶

To illustrate the effect of free carriers on the properties of our photonic crystal, we calculated the dependence of the photonic band structure on the plasma frequency. The Drude form of the dielectric function allows a plane-wave expansion of Maxwell's equations to be cast in the form of a standard eigenvalue equation.²⁹ We performed calculations for our structure with plasma frequencies in the range $0 < \omega_p a / 2\pi c < 1$ and found that 400 plane waves provided sufficient convergence.

The photonic band structure for the **E**- and **H**-polarized bands (electric-field polarized parallel and perpendicular to pore axis, respectively) and the dependence of the band-edge frequencies on the plasma frequency is shown in Fig. 2. All band-edge frequencies are blue shifted with increasing plasma frequency. The magnitude of the band-edge shift depends on both the mode frequency and the concentration of the mode energy in the silicon. The two-dimensional photonic band gap near 1.4 μm (indicated by the dashed line in Fig. 2) closes completely for plasma frequencies greater than $\omega_p = 0.57 \times 2\pi c/a$ (corresponding to $N = 2.3 \times 10^{20} \text{ cm}^{-3}$ for our material).

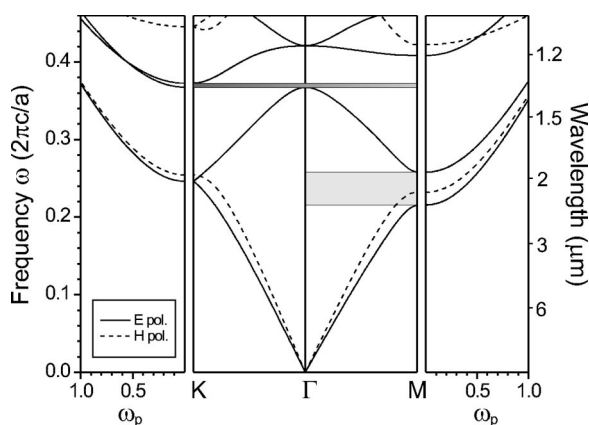


FIG. 2. Band structure of two-dimensional photonic crystal and dependence of band-edge frequencies on the plasma frequency ω_p , assuming a lossless dielectric function. The radius to pitch ratio is 0.411 and the wavelength scale is calculated assuming a pitch of 500 nm. The plasma frequency is given in units of $2\pi c/a$. Also shown are the complete two-dimensional band gap (narrow rectangle) and the stop band investigated in the experiment (wide rectangle).

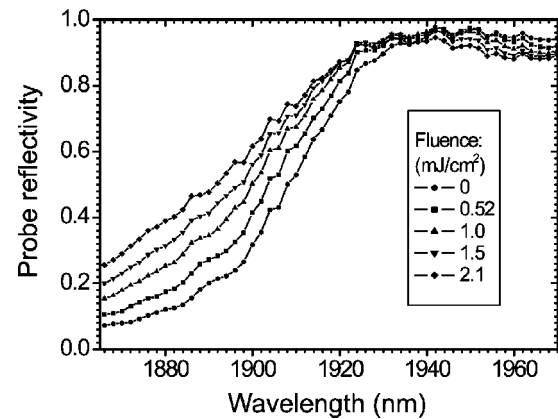


FIG. 3. **E**-polarized reflectivity of photonic crystal in Γ - M direction in vicinity of high-frequency fundamental band edge, and its dependence on pump fluence.

To observe the effects of carriers on the photonic band structure, we performed ultrafast pump and probe experiments using an optical parametric amplifier system pumped by a 800 nm, Ti:sapphire regenerative amplifier with a pulse repetition rate of 250 kHz. The system was configured to produce collinearly propagating **E**-polarized probe pulses near 1.9 μm (resonant with the high-frequency side of the first band gap) and **H**-polarized pump pulses at 800 nm, each with a width of approximately 300 fs. The probe was focused to a spot size of 30 μm , within the 90- μm spot size of the pump beam. The reflectivity spectrum was measured with a monochromator and a pyroelectric detector. A variable delay in the pump path allowed for the probe reflectivity to be measured as a function of time delay.

The probe reflection spectrum and its dependence on the pump pulse fluence is shown in Fig. 3 (measured with the probe delayed 13.5 ps from the pump, well beyond initial reflectivity transients). The unpumped sample reflectivity has a maximum value of 0.97 in the band gap, indicating high surface quality. The spectra are clearly blue shifted with increasing pump fluence, consistent with the Drude model discussed above. A maximum shift of $31 \pm 1 \text{ nm}$ is observed for a pump fluence of $2.1 \pm 0.4 \text{ mJ cm}^{-2}$. This shift spans nearly 10% of the unpumped crystal stop band. The steepness of the band-edge facilitates the observation of large differential reflectivities, in excess of 250% for the maximum pump fluence, although this steepness changes with fluence because of spatial inhomogeneity in the plasma with depth (see below). The reflectivity within the stop gap remains above 0.90 at the maximum pump fluence, indicating that absorption has a negligible effect on reflectivity.

The temporal evolution of the band-edge shift was observed by measuring the reflectivity of the photonic crystal while varying the delay between the pump and the probe pulses. The observed dependence is shown in Fig. 4, where the differential reflectivity is plotted as function of the probe delay for a pump pulse fluence of 1.3 mJ cm^{-2} at a probe wavelength of $\lambda = 1900 \text{ nm}$. The differential reflectivity increases with a rise time of approximately 400 fs, consistent with pump and probe pulse widths. There is also a residual rise of the reflectivity which occurs on a time scale of 2–3

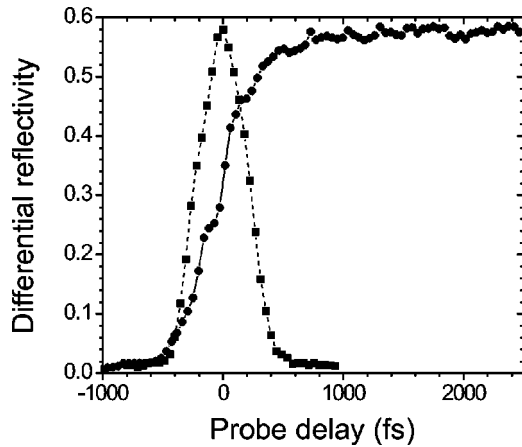


FIG. 4. Dependence of differential reflectivity ($\Delta R/R$) on probe delay for $\lambda = 1900$ nm and a pump fluence of 1.3 mJ cm^{-2} (solid). Also plotted is pump and probe cross correlation (dashed, arbitrary units).

ps; this is attributed to carrier cooling effects. As the carriers cool, their effective mass decreases, raising the Drude contribution to the dielectric constant and hence the reflectivity. The subsequent plateau was observed to be constant over the 70-ps delay range of the experiment. The constant plateau is consistent with the >1 ns expected carrier recombination lifetime of bulk silicon, governed by Auger recombination^{30,31} and surface recombination. The recombination lifetime can be reduced to approximately a picosecond via the introduction of radiation-induced defects or other nonradiative traps (e.g., as was done with other materials using ion implantation of oxygen in silicon on sapphire¹⁶ and low-temperature grown¹⁷ GaAs).

The observed dependence of the band-edge shift on the pump fluence fits very well with the linear behavior predicted by the plane-wave model. By fitting the maximum observed shift with the calculated shift, we obtained a relationship between the measured pump fluence and the excited carrier density. The inferred density fell in the range $(0.2 < N < 1.9) \times 10^{19} \text{ cm}^{-3}$ for the pump fluences used in the experiment. Using the fitted relationship between the density and the pump fluence, the effective pump absorption depth can be calculated via the relation $N = F(1 - R)/(E_p l)$, where F is the pump fluence, R is the pump reflectivity (measured to be 0.56), E_p is the pump photon energy, and l is the effective pump absorption depth. This relation gives $l = 2.0 \pm 0.4 \mu\text{m}$, which is five times smaller than that of bulk silicon.³³ The shallower absorption depth is attributed to a lower group velocity of the photonic band at 800 nm compared to that of bulk Si. The pump energy is therefore absorbed within approximately three crystal rows (one crystal row in the Γ -M direction has a length of $\sqrt{3}a = 866$ nm), leading to a carrier density that is spatially inhomogeneous.

We note that this depth could be extended by pumping with a wavelength closer to the electronic band edge of silicon, where the pump absorption depth is much larger.

The spatially inhomogeneous plasma, and the resulting depth dependence of the photonic band edge, accounts for important features of the reflectivity spectrum. When the crystal is not pumped, light with a wavelength below approximately 1880 nm (significantly below the band edge in Fig. 3) is partially reflected via the impedance mismatch at the crystal surface. Although most of the light couples to a propagating mode and probes the entire crystal, the reflected light only probes the surface layer of the crystal. However, when the wavelength is inside the stop band ($\lambda \geq 1940$ nm), all of the light is reflected due to the coherent superposition of an infinite number of backscattered waves from deep within the crystal. Therefore, as the wavelength increases toward the band edge, the reflection mechanism changes from impedance mismatch to Bragg scattering, and the *reflected* light probes deeper regions of the crystal.

The consequence for our inhomogeneously pumped crystal is that the short-wavelength reflectivity probes the highly pumped surface region, resulting in a large spectral shift. However, as the wavelength increases and crosses the blue shifted band edge of the pumped crystal, the reflected light penetrates deeper into the crystal. In fact, some of the deeply penetrating waves couple to the propagating modes of the weakly pumped part of the crystal, resulting in a lower reflectivity and a smaller shift. This effect is clearly seen in Fig. 3, where the shift is large for short wavelengths but decreases as the wavelength increases toward the band edge. This observation validates measuring the blue shift near the bottom of the peak, where the efficiently pumped surface layers are being probed. The qualitative explanation given above was theoretically verified using a one-dimensional transfer-matrix model of the inhomogeneously pumped photonic crystal. The results, to be presented elsewhere, correctly reproduce the observed spectral shape for an absorption depth of three layers, confirming our model.

In summary, we have demonstrated ultrafast all-optical tuning of the band gap of a silicon photonic crystal using free-carrier injection. Our results indicate that optical free-carrier injection offers a practical means of controlling the band edges and photon densities of states on ultrafast time scales. The use of free carriers to control the properties of photonic crystals clearly presents many exciting opportunities for ultrafast all-optical switching in the near future.

We thank Serguei Grabtchak and Jessica Mondia for useful discussions and S. Matthias, F. Müller, and A. Birner for technical assistance. Two of the authors (S.W.L. and H.V.D.) gratefully acknowledge the financial support of the Natural Sciences and Engineering Research Council of Canada and Photonics Research Ontario.

*Present address: NovX Systems, Inc., 185 Renfrew Drive, Markham, Ontario L3R 6G3, Canada. Email address: stephen@novxsystems.com

¹E. Yablonovitch, Phys. Rev. Lett. **58**, 2059 (1987).

²S. John, Phys. Rev. Lett. **58**, 2486 (1987).

³*Photonic crystals and light localization in the 21st century*, edited by C. Soukoulis (Kluwer Academic Publishers, Boston, 2001).

⁴J. D. Joannopoulos, R. D. Meade, and J. N. Winn, *Photonic Crystals*

- tals: Molding the Flow of Light* (Princeton University Press, Princeton, 1995).
- ⁵S. Noda, A. Chutinan, and M. Imada, *Nature* (London) **407**, 608 (2000).
- ⁶A. Blanco *et al.*, *Nature* (London) **405**, 437 (2000).
- ⁷E. Chow *et al.*, *Opt. Lett.* **26**, 286 (2001).
- ⁸R.F. Cregan *et al.*, *Science* **285**, 1537 (1999).
- ⁹H. Kosaka *et al.*, *Phys. Rev. B* **58**, R10 096 (1998).
- ¹⁰H.P. Schriemer *et al.*, *Phys. Rev. A* **63**, 011801 (2001).
- ¹¹K. Busch and S. John, *Phys. Rev. Lett.* **83**, 967 (1999).
- ¹²K. Yoshino *et al.*, *Jpn. J. Appl. Phys., Part 2* **38**, L961 (1999).
- ¹³S.W. Leonard *et al.*, *Phys. Rev. B* **61**, R2389 (2000).
- ¹⁴D. Kang *et al.*, *Phys. Rev. Lett.* **86**, 4052 (2001).
- ¹⁵M.I. Gallant and H.M. van Driel, *Phys. Rev. B* **26**, 2133 (1982).
- ¹⁶F.E. Doany, D. Grischkowsky, and C.-C. Chi, *Appl. Phys. Lett.* **50**, 460 (1987).
- ¹⁷F.W. Smith *et al.*, *Appl. Phys. Lett.* **54**, 890 (1989).
- ¹⁸P. Halevi and F. Ramos-Mendieta, *Phys. Rev. Lett.* **85**, 1875 (2000).
- ¹⁹S. Susa, *Jpn. J. Appl. Phys., Part 1* **39**, 6288 (2000).
- ²⁰A. Haché and M. Bourgeois, *Appl. Phys. Lett.* **77**, 4089 (2000).
- ²¹A. Chelnikov *et al.*, *Electron. Lett.* **34**, 1965 (1998).
- ²²H. M. van Driel *et al.*, in *Tuning 2-D Silicon Photonic Crystals*, Mater. Res. Soc. Proc. No. 722 (Materials Research Society, Pittsburgh, 2002), L3.1.
- ²³U. Grüning *et al.*, *Appl. Phys. Lett.* **68**, 747 (1996).
- ²⁴A. Birner *et al.*, *Advan. Mater.* **13**, 377 (2001).
- ²⁵J. Schilling *et al.*, *Opt. Mater.* **17**, 7 (2001).
- ²⁶Using an effective mass²⁷ of $m^* = 0.16m_0$ (where m_0 is the electron mass), a momentum relaxation time of $\tau \sim 100$ fs, and an intervalence band cross section²⁸ of 10^{-17} cm², the magnitude of the free-carrier induced imaginary term¹⁵ in the dielectric function is approximately an order of magnitude smaller than that of the real term.
- ²⁷O. Madelung, *Semiconductors-Basic Data* (Springer, New York, 1996), p. 11.
- ²⁸L.M. Lambert, *Phys. Status Solidi A* **11**, 461 (1972).
- ²⁹V. Kuzmiak, A.A. Maradudin, and F. Pincemin, *Phys. Rev. B* **50**, 16 835 (1994).
- ³⁰A. Haug and W. Schmid, *Solid-State Electron.* **25**, 665 (1982).
- ³¹Using an Auger coefficient of 1.9×10^{-31} for silicon,³² the minimum recombination lifetime (corresponding the maximum density of 2.0×10^{19} cm⁻³) is predicted to be approximately 13 ns, consistent with the observed time-independent plateau in the picosecond regime.
- ³²J. Dziejwior and W. Schmid, *Appl. Phys. Lett.* **31**, 346 (1977).
- ³³W.C. Dash and R. Newton, *Phys. Rev.* **99**, 1151 (1955).